

RESEARCH ARTICLE

High Frequency Hearing Loss and Hyperactivity in DUX4 Transgenic Mice

Abhijit Dandapat¹, Benjamin J. Perrin², Christine Cabelka³, Maria Razzoli⁴, James M. Ervasti², Alessandro Bartolomucci⁴, Dawn A. Lowe³, Michael Kyba^{1*}

1 Lillehei Heart Institute and Department of Pediatrics, University of Minnesota, Minneapolis, 55455, United States of America, **2** Department of Biochemistry, University of Minnesota, Minneapolis, 55455, United States of America, **3** Program in Physical Medicine and Rehabilitation, University of Minnesota, Minneapolis, 55455, United States of America, **4** Department of Integrative Biology and Physiology, University of Minnesota, Minneapolis, 55455, United States of America

* kyba@umn.edu



OPEN ACCESS

Citation: Dandapat A, Perrin BJ, Cabelka C, Razzoli M, Ervasti JM, Bartolomucci A, et al. (2016) High Frequency Hearing Loss and Hyperactivity in DUX4 Transgenic Mice. PLoS ONE 11(3): e0151467. doi:10.1371/journal.pone.0151467

Editor: Frédérique Magdinier, INSERM UMR S_910, FRANCE

Received: July 7, 2015

Accepted: February 29, 2016

Published: March 15, 2016

Copyright: © 2016 Dandapat et al. This is an open access article distributed under the terms of the [Creative Commons Attribution License](https://creativecommons.org/licenses/by/4.0/), which permits unrestricted use, distribution, and reproduction in any medium, provided the original author and source are credited.

Data Availability Statement: All relevant data are within the paper.

Funding: This work was supported by the following agencies and foundations: National Institute of Arthritis and Musculoskeletal and Skin Diseases R01 AR055685 (to M.K.) and R01 AR049899 (to J.E.); National Institute on Deafness and Other Communication Disorders R03 DC12354 (to B.P.); National Institute of Diabetes and Digestive and Kidney Diseases R01 DK102496 (to A.B.); National Institute on Aging R01 AG031743 (to D.L.); and The Bob and Jean Smith Foundation (to M.K.). The funders had no role in study design, data collection

Abstract

Facioscapulohumeral muscular dystrophy (FSHD) is caused by mutations leading to ectopic expression of the transcription factor DUX4, and encompasses both muscle-related and non-muscle phenotypes. Mouse models bearing this gene represent valuable tools to investigate which pathologies are due to DUX4 expression, and how DUX4 leads to these pathologies. The iDUX4(2.7) mouse contains an X-linked doxycycline-inducible DUX4 gene that shows low level basal expression in the absence of doxycycline, leading to male lethality, generally in embryo, but always before 8 weeks of age. Here, we describe additional non-muscle phenotypes in this animal model. We find that iDUX4(2.7) female carriers are extremely hyperactive, spending large amounts of time ambulating and much less time resting. Rare 3-week old males, although hypophagic, runted and extremely fragile, are capable of high activity, but show periods of catatonic torpor in which animals appear dead and respiration is virtually absent. We also examine a non-muscle phenotype of interest to FSHD, high frequency hearing loss. We find that young iDUX4(2.7) females are significantly impaired in their ability to hear at frequencies above 8 kHz. These phenotypes make the iDUX4(2.7) mouse an attractive model in which to study non-muscle activities of DUX4.

Introduction

Facioscapulohumeral muscular dystrophy (FSHD) is a genetic disease caused by ectopic expression of an unusual double homeodomain transcription factor, DUX4. The proximate cause of this ectopic expression is an alteration in the chromatin that normally forms at the DUX4 locus, converting it from heavily methylated DNA bearing histone marks of heterochromatin or gene repression to relatively demethylated DNA bearing histone marks associated with gene expression, leading to transcription of the locus [1–4]. The *DUX4* gene is embedded in a macrosatellite repeat array, referred to as *D4Z4* and which is normally present in 50+ copies [5]. The ultimate cause of the chromatin changes that lead to its expression is a complex

and analysis, decision to publish, or preparation of the manuscript.

Competing Interests: The authors have declared that no competing interests exist.

interplay between repeat copy number and second site mutations or allelic differences that affect the activity of chromatin regulators: in most cases, the *D4Z4* array is contracted to 10 or fewer copies; fewer copies of *D4Z4* predispose to transcription [6, 7]. In some cases, transcription/FSHD can occur with >10 repeats, in which the disease is referred to as FSHD2, although clinically indistinguishable from FSHD1 [4]. Mutation of the chromatin protein *SMCHD1* promotes expression of the array, and causes a large number of cases of FSHD2 [8], and genetic background, specifically allelic differences of other genes, presumably chromatin regulators, also influences expression, particularly in the “gray area” of 7–10 repeats [9]. In addition to variation in array number, the sequence downstream of the array comes in multiple alleles, some of which encode a functional polyA, and FSHD only occurs on such alleles [10].

The protein encoded by the locus is expressed at very low frequencies in *ex vivo* cultured cells from FSHD-affected individuals [11, 12]. Forced expression studies in cells *in vitro* have shown that low levels of *DUX4* interfere with *MyoD* transcription, impair myogenesis *in vitro*, and sensitize cells to oxidative stress [13], while high levels of expression lead to cell death [13, 14]. *DUX4* binds an AT-rich motif [15, 16] and induces many target genes [13, 15, 17] but a clear explanation for how these molecular events drive muscle wasting is lacking. Three *DUX4* transgenic mouse models have been described to date. In the first two, human genomic DNA constructs carrying permissive alleles, one from a two-unit FSHD case and another from a 12 unit control, were integrated randomly to generate high copy and a low copy strains. Neither mouse showed any major pathology, however the low copy strain showed low levels of *DUX4* expression in some tissues, including in cells from skeletal muscle [18]. In the third model, referred to as iDUX4(2.7), a 2.7 kb fragment of the *DUX4* gene including the *DUX4* ORF and downstream untranslated sequence was integrated into euchromatic DNA on the X-chromosome, under the regulation of a doxycycline-inducible promoter [19]. In the absence of doxycycline, this transgene showed extremely low levels of basal expression, which caused very strong phenotypes, resulting in very low numbers of live-born males, and male-specific lethality. Females were less affected because of X-inactivation, and although somewhat runted and displaying a skin phenotype, the females were able to propagate the strain by breeding with wild type (WT) males. While muscle tissues from affected males showed no obvious signs of dystrophy prior to their early demise (between 2–8 weeks), they were composed of smaller-diameter fibers, and *ex vivo* cultured myoblasts showed a moderate decrease in proliferation rate. When the *DUX4* transgene was switched on by doxycycline treatment, myoblast differentiation was impaired *in vitro* and skeletal muscle regeneration was impaired *in vivo*. One of the interesting potentially FSHD-related non-muscle phenotypes seen in this mouse model was a retinal vascular telangiectasia. Most FSHD-affected individuals suffer a similar subclinical retinal vasculopathy involving vessel tortuosity and occlusions [20, 21].

In the present study, we have investigated additional phenotypes in these iDUX4(2.7) mice. Because we noted that these animals were highly active, and often had reduced adipose tissue, we investigated their activity levels, metabolism and heat production compared to WT mice. In addition, because high frequency hearing loss is reported as one of the common non-muscle manifestations of FSHD [21], particularly in cases with very short *D4Z4* arrays [22], we investigated hearing loss in these mice.

Results and Discussion

The doxycycline-inducible *DUX4* transgene was targeted into a site on the X-chromosome, therefore the pathological phenotypes are less severe in females than in males [19]. Phenotypes are not due to insertional mutagenesis, as the insertion site is in intergenic DNA upstream of the *HPRT* gene, which is functional as it was used for selection. X-inactivation mitigates the

phenotype in females, as seen most clearly in the skin, where alopecia presents in stripes, typical of Lyonization of X-linked coat color genes in heterozygotes [23], rather than throughout the skin as in males. In other tissues, for example muscle, cells that have inactivated the wild-type (WT) X are apparently selected against during development. Cells from adult female muscle showed almost exclusive inactivation of the DUX4-bearing X [19]. This tissue mosaicism and selection for inactivation of the DUX4-bearing X mean that females present a filtered phenotype. Unfortunately, iDUX4(2.7) males are born alive at only one fifth of the expected Mendelian ratio, they are extremely runted, and rarely live for more than six weeks. These caveats mean that certain phenotypes present most strongly in males, while others are impossible or not meaningful to evaluate in males due to their truncated lifespan, and are thus evaluated in females.

iDUX4(2.7) males alternate between periods of elevated respiration and episodes of catatonic torpor

At weaning, iDUX4(2.7) male mice showed low body size and a high level of variation in body fat (Fig 1). This compelled us to study their metabolism using indirect calorimetry on mice housed for 48 hours in environmental chambers at weaning age. Over these 48 hours, the iDUX4 male weanlings showed a peculiar metabolic phenotype comprised of phases of high VO_2 , VCO_2 , and activity values, interspersed with periods of sudden inactivity coupled with precipitous decline in respiratory exchanges (Fig 2). Most remarkably, after these catatonic torpor-like episodes (prolonged immobility, minimal VO_2 and VCO_2) each iDUX4(2.7) animal showed a return to active metabolic function even if they eventually died before the end of the 2 days of recordings (Fig 2). In spite of these phases of prolonged immobility, when the iDUX4(2.7) males were active, they often showed peaks of much greater than normal activity (Fig 2C). Interestingly, during the 2 days in the calorimetry chambers, the iDUX4(2.7) mice also showed lower food intake compared to WT (Fig 1E and 1F), which may implicate food intake as a primary driver of the runting phenotype.

For statistical analysis of metabolic parameters, because many iDUX4(2.7) mice died before the end of the 48 h observation, we compared the values over a one hour period of recording after introducing the mice in the metabolic chambers, and in which no animals were experiencing a catatonic torpor-like episode (these studies exclude one mouse that died before starting the indirect calorimetry). We also evaluated the maximum recorded values for VO_2 , VCO_2 and activity over the course of the entire 48 h observation. iDUX4(2.7) subjects showed increased maximal VO_2 compared to WT (Fig 2G) as well as a slight, albeit not significant, increase for all other parameters (Fig 2). Visual inspections of the brown adipose tissue (BAT) showed a small but proportionally normal organ considering the small body size of the DUX4 mice.

We considered the possibility that these metabolic abnormalities were due to deregulated or hyperactive adaptive thermogenesis. We therefore tested whether rearing animals at thermoneutrality (30°C, which is mouse thermoneutrality [24]) would ameliorate the lethal phenotype in males. We acclimatized breeding pairs at thermoneutrality and evaluated frequency and health of live-born male progeny inheriting the *DUX4* transgene. Contrary to the hypothesis, the phenotype was not improved at thermoneutrality. Male pups were still born at much lower than Mendelian ratios, and most died before 3 weeks (Tables 1 and 2). No male carriers survived beyond 6 weeks.

Due to the low body fat and food intake it is conceivable that the iDUX4(2.7) males die because of insufficient stored nutrients. The metabolic phenotype of these male animals resembles conditions of prolonged fasting [25, 26], H_2S exposure [27] as well as other mutant strains characterized by small body size and impaired feeding behavior [28, 29]. A type of torpor can

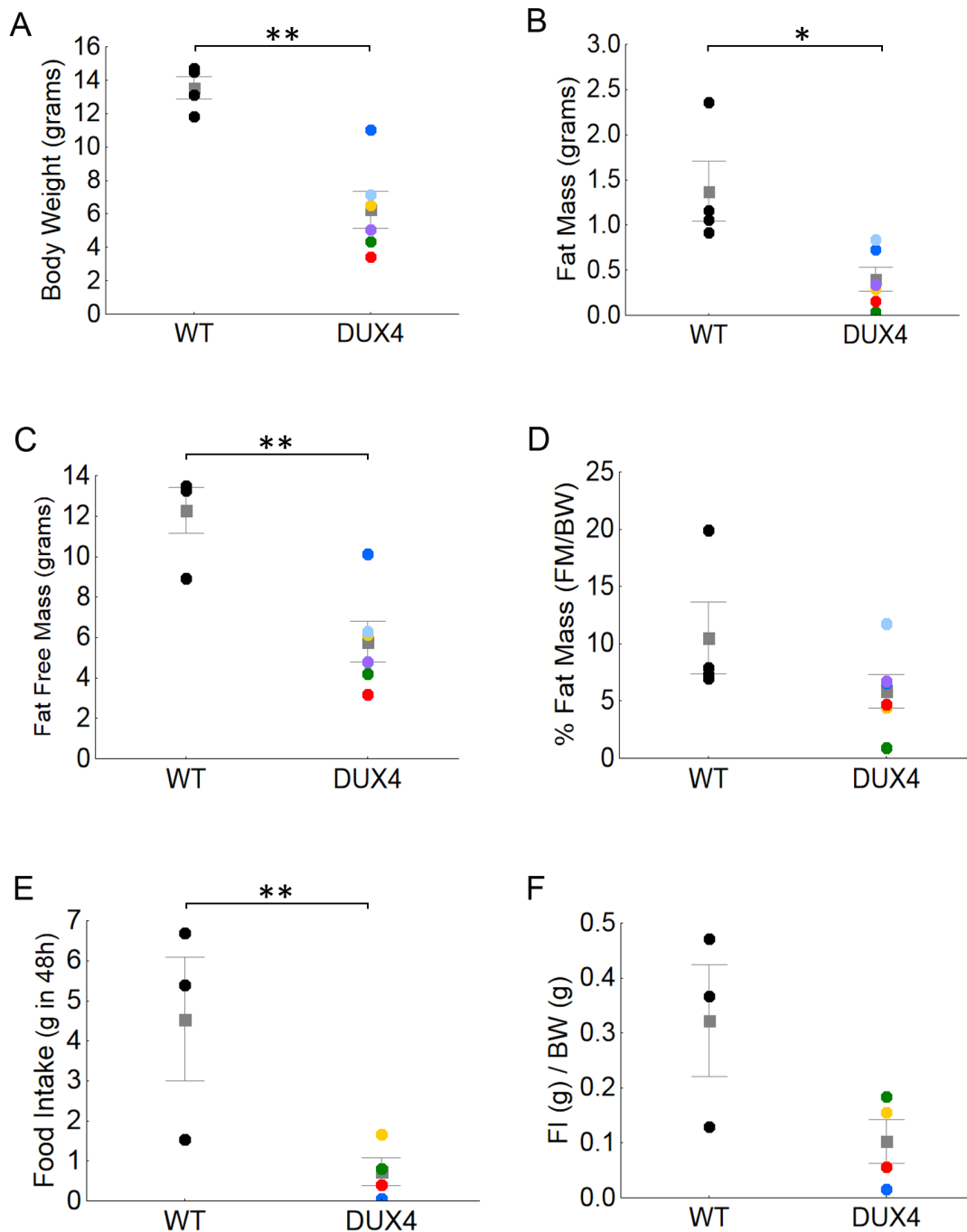


Fig 1. Metabolic parameters in iDUX4 male mice. **A)** Body weight ($t_8 = 4.9, p < 0.01$). Mean is shown as a gray box; error bars indicate SEM; values for individual mice are indicated by colored symbols. **B)** Fat mass ($t_8 = 3.2, p < 0.05$). **C)** Fat free mass ($t_8 = 4.2, p < 0.01$). **D)** % Fat mass. For A-D, $n = 4$ WT and 6 iDUX4. **E-F)** Food intake during the 48h in the indirect calorimetry chambers expressed in grams ($t_5 = 2.8, p < 0.05$) and grams relative to body weight. * $P < 0.05$. ** $P < 0.01$. Color coding identifies individual DUX4 mice. $N = 3$ WT and 4 DUX4.

doi:10.1371/journal.pone.0151467.g001

be induced by starvation, however such torpor is characterized by periods of inactivity and reduced respiration, not a virtual absence of respiration as was observed in this study. Indeed, based on metabolic parameters, the catatonic mice in this study were presumed to have died, and their recovery considered remarkable when first observed.

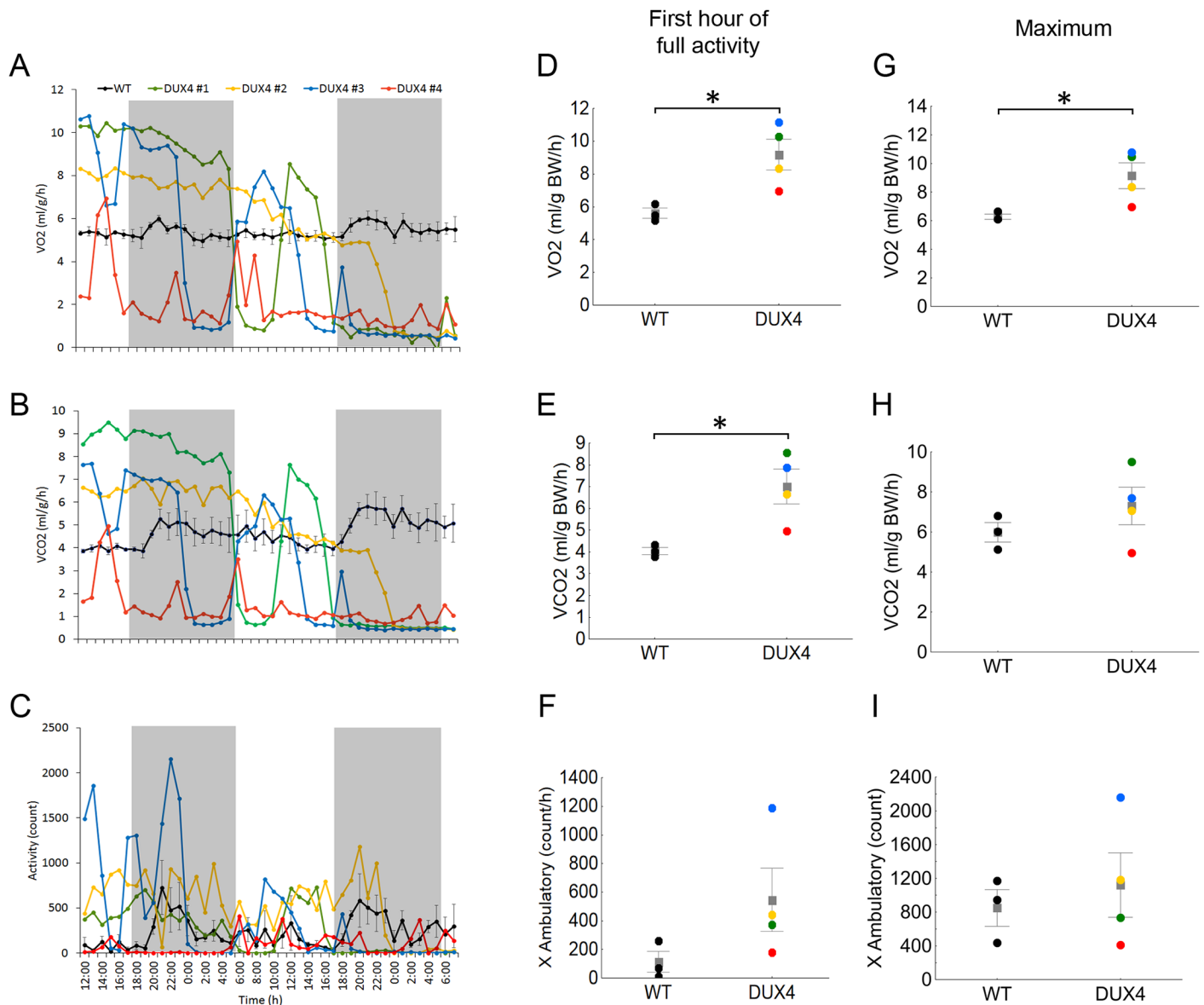


Fig 2. VO₂, VCO₂ and locomotor activity in DUX4 male mice at weaning. A-C) Hourly average of VO₂, VCO₂ and locomotor activity measured in the indirect calorimetry chambers over 48h. WT mice are represented by group average, while DUX4 mice are presented individually due to the extreme inter-individual and temporal variability in the metabolic parameters (mice went into and came out of a motionless, energetically negligible state several times over the course of recording). Color coding identifies individual DUX4 animals (colors are consistent with Fig 1). D-F) Group averages of metabolic parameters measured during the first hour in which animals showed activity after introducing the animals in the indirect calorimetry chambers. VO₂ ($t_5 = 3.1$, $p < 0.05$), VCO₂ ($t_5 = 3.1$, $p < 0.05$). G-I) Maximum values recorded during the 48h of recording. (VO₂ max: $t_5 = 2.7$, $p < 0.05$); * $P < 0.05$. For A-I, $n = 3$ WT and 4 iDUX4.

doi:10.1371/journal.pone.0151467.g002

DUX4(2.7) females are hyperactive

The iDux4(2.7) female mice show a slightly reduced size, but are not severely runted, and they remain relatively healthy and fertile. However, in the course of routine animal husbandry we observed that they were noticeably more jumpy and were often seen spinning. We therefore performed a detailed study of their movements in which 4 month old females and their litter-mate female controls were analyzed over 24 hours using activity-monitoring cages. This revealed that the female iDUX4(2.7) mice are indeed extremely hyperactive, including

Table 1. Viability of male mice at room temperature.

Litters	Live Born Males		Males Surviving to 3 Weeks	
	WT Males	Dux4 Males	WT Survived	Dux4 Survived
#1	4	2	4	
#2	5	1	5	1
#3	4	1	4	
#4	4		4	
#5	4	3	4	
#6	4	1	4	
#7	3		3	
#8	2	1	2	1
Total	30	9	30	2
Ratio		30%	100%	22%

Summary data from eight litters born at room temperature. Live-born ratios indicate frequency relative to expected (WT males). 3 week survival ratios indicate the frequency of live-born animals surviving to 3 weeks of each genotype.

doi:10.1371/journal.pone.0151467.t001

abnormal behavioral activities like spinning (Fig 3A). Although the number of ambulatory episodes was not different, the iDUX4(2.7) mice spent much more time engaged in each ambulation and covered more distance (Fig 3A–3C). In addition, comparing active time to time spent resting revealed that the iDUX4 animals spent on average over 7 hours of each day being active compared to < 4h for historical [30] as well as littermate controls (Fig 3D, p = 0.014).

Hyperactivity has not been described in humans with FSHD. We speculated previously [19] that the iDUX4(2.7) mice might represent the extreme high end of a spectrum of phenotypes that arise due to elevated levels of DUX4 expression, because this allele is not subject to repeat-induced silencing (being only a single D4Z4 unit) and because it is inserted into relatively active euchromatin, rather than subtelomeric heterochromatin. Thus, metabolic abnormalities and hyperactivity may require higher levels of DUX4 than are ever seen in FSHD in humans, or they may be novel mouse-specific effects of DUX4.

Table 2. Viability of male mice at thermoneutrality.

Litters	Live Born Males		Males Surviving to 3 Weeks	
	WT Males	Dux4 Males	WT Survived	Dux4 Survived
#1	4	1	4	
#2	3	2	3	
#3	3	1	3	1
#4	4		4	
#5	2	1	2	
#6	4	1	4	1
#7	2	1	2	1
#8	3		3	
Total	25	7	25	3
Ratio		28%	100%	43%

Summary data, as in Table 1, from eight litters born at thermoneutrality.

doi:10.1371/journal.pone.0151467.t002

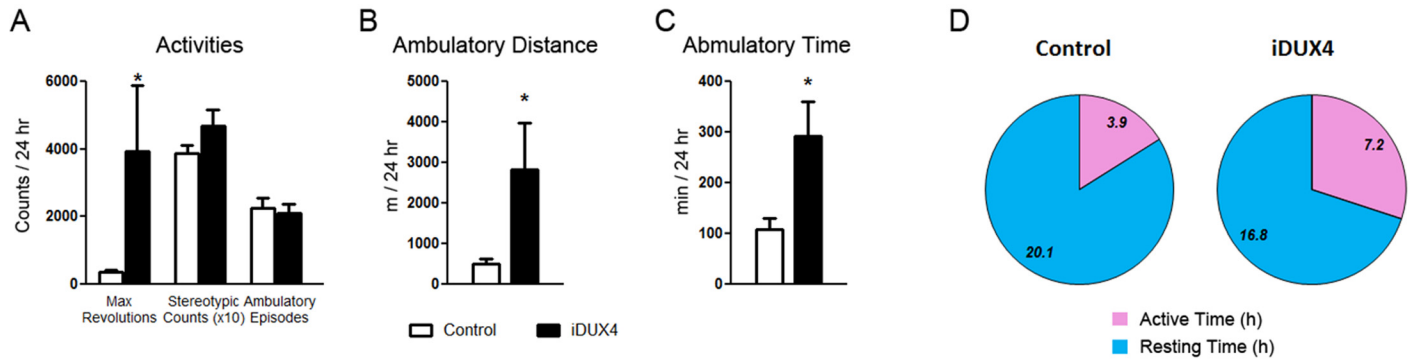


Fig 3. Activity measurements of DUX4 female mice. **A)** Measurements for various types of activity identifiable in activity monitoring cages. For these studies, N = 6 iDUX4(2.7) females and 6 littermate controls. **B)** Total ambulatory distance over 24 hours. **C)** Total ambulatory time over 24 hours. **D)** Comparison of resting vs. active time. Differences between control and iDUX4 animals were significant to $p = 0.014$.

doi:10.1371/journal.pone.0151467.g003

DUX4(2.7) females show high frequency hearing loss

Because one of the principal non-muscle phenotypes associated with FSHD in humans is high frequency hearing loss [21, 31, 32], we sought to evaluate whether iDUX4(2.7) animals had any hearing abnormalities. Young (between 1 and 5 months of age) female transgenic animals and their WT sibling controls were exposed to 1 msec sonic bursts of increasing amplitude over a range of frequencies and their auditory brainstem response was monitored (Fig 4). This revealed a clear reduction in sensitivity to sound at frequencies greater than 8 kHz. These data are quite interesting from the perspective of non-muscle phenotypes in FSHD, and they suggest

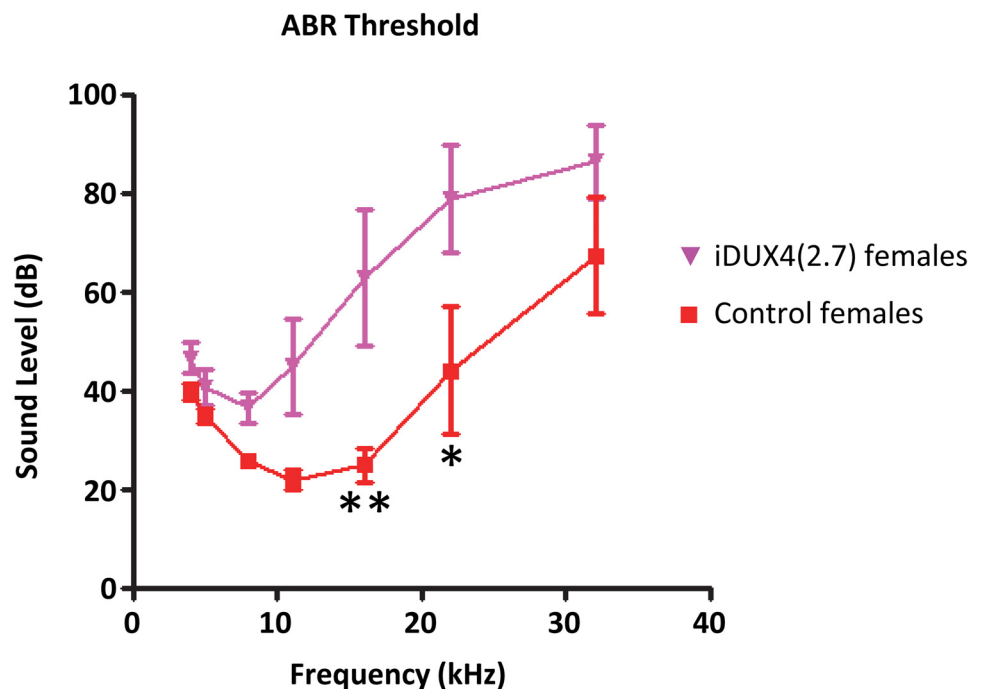


Fig 4. Hearing loss in iDUX4 mice. Auditory brainstem response (ABR) is shown at each frequency indicated over a range of sound levels. N = 5 iDUX4(2.7) and 5 WT littermate control female mice. * $p < 0.05$, ** $p < 0.01$.

doi:10.1371/journal.pone.0151467.g004

that misexpression of DUX4 in cells outside of muscle may be responsible for certain pathologies seen in FSHD. Whether this phenotype is homologous to the hearing loss in FSHD patients is difficult to say. Ultimately, the hearing loss in humans and mice are both caused by the *DUX4* gene, but elucidating the mechanism of hearing loss in the iDUX4(2.7) mice will require further study.

Conclusions

In this study, we document additional dox-independent (i.e. seen in the absence of Dox) phenotypes of the iDUX4(2.7) mice. These include a phenotype of clear relevance to FSHD (hearing loss), as well as phenotypes for which there is no known cognate in this patient population (hyperactivity and periods of apparent complete metabolic inactivity accompanied by immobility).

Materials and Methods

Mice were maintained in accordance with the Guide for Care and Use of Laboratory Animals of the NIH and the University of Minnesota Institutional Animal Care and Use Committee approved this study. Female iDUX4(2.7) carriers were bred with WT males or with males carrying the Rosa26-rtTA2Sm2 transgene [33].

Auditory Brainstem Response (ABR)

ABR were performed as described previously [34]. Prior to testing, mice were anaesthetized with avertin and scalp potentials were recorded via subdermal electrodes on the head. Stimuli consisted of symmetrically shaped tone bursts 1 millisecond in duration with 300-microsecond raised cosine ramps and were delivered to a calibrated magnetic speaker. ABRs were bandpass filtered between 0.03 and 10 kHz; signals were amplified 20,000 times, digitized using a 20,000-kHz sampling rate, and subjected to artifact rejection. ABR waveforms were collected for frequencies between 4 kHz and 32 kHz at half octave steps, starting at suprathreshold levels and decreasing in 5 dB steps to a level 10 dB below the threshold. Stacked waveforms were compared and the lowest level of stimulation that evoked an unambiguous ABR waveform was designated as the threshold.

Activity monitoring cages

Cage activities were measured over 24-h using open field activity chambers (Med Associates Inc., St. Albans, VT) as in Greising et al [30] except for the following. To account for the small size of Dux4 mice, the height of the top horizontal beam was lowered to 2.5 cm and the box size which differentiates stereotypic movement from ambulation was set to “2” (3.2 cm²).

Metabolic phenotype

Body composition was measured with Echo-MRI (Echo Medical Systems). After body composition measure mice were individually placed in the OxyMax Comprehensive Lab Animal Monitoring System (Columbus Instruments). Oxygen consumption (VO₂), carbon dioxide production (VCO₂) and ambulatory activity were measured over the course of 2 days. Respiratory exchange ratio (RER, or Respiratory quotient) and heat production were calculated but not reported because the assumptions are not met in abnormal metabolic states [35–37]. VO₂ and VCO₂ were normalized over grams of body weight. Food intake was calculated from the difference between the food allocated to every mouse at the start of the recording and the amount of food that was left at the end of the recording. All experiments were performed at

the IBP Phenotyping Core Facility, University of Minnesota. Data were analyzed with unpaired t-test.

Assessing survival ratios

Litters born at room temperature and 30°C were evaluated daily. Normal mice were weaned at 3 weeks, while runts were kept with their mothers indefinitely. Humane endpoints were used: mice were euthanized by CO₂ asphyxiation if they were found to be moribund, i.e. not moving at two different evaluations several hours apart.

Statistics

Data sets for all experimental and control groups were evaluated for normality (Kolmogorov-Smirnov test) and in where found consistent with normal distribution (most cases), Student's T-test was used to determine significance of differences between group means, with an assumption of difference at $p < 0.05$. Mann-Whitney U Tests were used to analyze data that were not distributed normally (cage activity parameters: max revolutions and ambulatory distance) with significance also set at $p < 0.05$.

Acknowledgments

This work was supported by NIH grants R01 AR055685 (to M.K.), R03 DC12354 (to B.P.), RO1 AR049899 (to J.E.), R01 DK102496 (to A.B.) and R01 AG031743 (to D.L.). The metabolic experiments were conducted at the IBP Phenotyping Core, University of Minnesota. We thank Jarod A. Call for help with activity cages. We thank the Bob and Jean Smith Foundation for their generous support.

Author Contributions

Conceived and designed the experiments: MK DL AB. Performed the experiments: AD BP MR CC. Analyzed the data: AD BP MR CC JE DL AB MK. Wrote the paper: AD BP DL AB MK.

References

1. Gabellini D, Green MR, Tupler R. Inappropriate gene activation in FSHD: a repressor complex binds a chromosomal repeat deleted in dystrophic muscle. *Cell*. 2002; 110(3):339–48. PMID: [12176321](#).
2. Zeng W, de Greef JC, Chen YY, Chien R, Kong X, Gregson HC, et al. Specific loss of histone H3 lysine 9 trimethylation and HP1gamma/cohesin binding at D4Z4 repeats is associated with facioscapulohumeral dystrophy (FSHD). *PLoS genetics*. 2009; 5(7):e1000559. Epub 2009/07/14. doi: [10.1371/journal.pgen.1000559](#) PMID: [19593370](#).
3. van Overveld PG, Lemmers RJ, Sandkuijl LA, Enthoven L, Winokur ST, Bakels F, et al. Hypomethylation of D4Z4 in 4q-linked and non-4q-linked facioscapulohumeral muscular dystrophy. *Nat Genet*. 2003; 35(4):315–7. PMID: [14634647](#).
4. de Greef JC, Lemmers RJ, van Engelen BG, Sacconi S, Venance SL, Frants RR, et al. Common epigenetic changes of D4Z4 in contraction-dependent and contraction-independent FSHD. *Hum Mutat*. 2009; 30(10):1449–59. Epub 2009/09/04. doi: [10.1002/humu.21091](#) PMID: [19728363](#).
5. Gabriels J, Beckers MC, Ding H, De Vriese A, Plaisance S, van der Maarel SM, et al. Nucleotide sequence of the partially deleted D4Z4 locus in a patient with FSHD identifies a putative gene within each 3.3 kb element. *Gene*. 1999; 236(1):25–32. Epub 1999/08/06. S0378-1119(99)00267-X [pii]. PMID: [10433963](#).
6. Wijmenga C, Hewitt JE, Sandkuijl LA, Clark LN, Wright TJ, Dauwerse HG, et al. Chromosome 4q DNA rearrangements associated with facioscapulohumeral muscular dystrophy. *Nat Genet*. 1992; 2(1):26–30. PMID: [1363881](#).
7. van Deutekom JC, Wijmenga C, van Tienhoven EA, Gruter AM, Hewitt JE, Padberg GW, et al. FSHD associated DNA rearrangements are due to deletions of integral copies of a 3.2 kb tandemly repeated unit. *Human molecular genetics*. 1993; 2(12):2037–42. PMID: [8111371](#).

8. Lemmers RJ, Tawil R, Petek LM, Balog J, Block GJ, Santen GW, et al. Digenic inheritance of an SMCHD1 mutation and an FSHD-permissive D4Z4 allele causes facioscapulohumeral muscular dystrophy type 2. *Nat Genet.* 2012; 44(12):1370–4. Epub 2012/11/13. doi: [ng.2454](https://doi.org/10.1038/ng.2454) [pii] doi: [10.1038/ng.2454](https://doi.org/10.1038/ng.2454) PMID: [23143600](https://pubmed.ncbi.nlm.nih.gov/23143600/).
9. Lemmers RJ, Goeman JJ, van der Vliet PJ, van Nieuwenhuizen MP, Balog J, Vos-Versteeg M, et al. Inter-individual differences in CpG methylation at D4Z4 correlate with clinical variability in FSHD1 and FSHD2. *Human molecular genetics.* 2014. Epub 2014/09/27. doi: [10.1093/hmg/ddu486](https://doi.org/10.1093/hmg/ddu486) PMID: [25256356](https://pubmed.ncbi.nlm.nih.gov/25256356/).
10. Lemmers RJ, van der Vliet PJ, Klooster R, Sacconi S, Camano P, Dauwerse JG, et al. A unifying genetic model for facioscapulohumeral muscular dystrophy. *Science.* 2010; 329(5999):1650–3. PMID: [20724583](https://pubmed.ncbi.nlm.nih.gov/20724583/). doi: [10.1126/science.1189044](https://doi.org/10.1126/science.1189044)
11. Snider L, Geng LN, Lemmers RJ, Kyba M, Ware CB, Nelson AM, et al. Facioscapulohumeral dystrophy: incomplete suppression of a retrotransposed gene. *PLoS genetics.* 2010; 6(10):e1001181. Epub 2010/11/10. doi: [10.1371/journal.pgen.1001181](https://doi.org/10.1371/journal.pgen.1001181) PMID: [21060811](https://pubmed.ncbi.nlm.nih.gov/21060811/).
12. Jones TI, Chen JC, Rahimov F, Homma S, Arashiro P, Beermann ML, et al. Facioscapulohumeral muscular dystrophy family studies of DUX4 expression: evidence for disease modifiers and a quantitative model of pathogenesis. *Human molecular genetics.* 2012; 21(20):4419–30. Epub 2012/07/17. doi: [10.1093/hmg/dds284](https://doi.org/10.1093/hmg/dds284) [pii] doi: [10.1093/hmg/dds284](https://doi.org/10.1093/hmg/dds284) PMID: [22798623](https://pubmed.ncbi.nlm.nih.gov/22798623/).
13. Bosnakovski D, Xu Z, Gang EJ, Galindo CL, Liu M, Simsek T, et al. An isogenetic myoblast expression screen identifies DUX4-mediated FSHD-associated molecular pathologies. *The EMBO journal.* 2008; 27(20):2766–79. Epub 2008/10/04. doi: [emboj2008201](https://doi.org/10.1038/emboj.2008.201) [pii] doi: [10.1038/emboj.2008.201](https://doi.org/10.1038/emboj.2008.201) PMID: [18833193](https://pubmed.ncbi.nlm.nih.gov/18833193/).
14. Kowaljow V, Marcowycz A, Anseau E, Conde CB, Sauvage S, Matteotti C, et al. The DUX4 gene at the FSHD1A locus encodes a pro-apoptotic protein. *Neuromuscul Disord.* 2007; 17(8):611–23. PMID: [17588759](https://pubmed.ncbi.nlm.nih.gov/17588759/).
15. Geng LN, Yao Z, Snider L, Fong AP, Cech JN, Young JM, et al. DUX4 activates germline genes, retroelements, and immune mediators: implications for facioscapulohumeral dystrophy. *Dev Cell.* 2012; 22(1):38–51. Epub 2012/01/03. S1534-5807(11)00523-5 [pii] doi: [10.1016/j.devcel.2011.11.013](https://doi.org/10.1016/j.devcel.2011.11.013) PMID: [22209328](https://pubmed.ncbi.nlm.nih.gov/22209328/).
16. Zhang Y, Lee JK, Toso EA, L JS., C SH., Slattery M, et al. DNA-binding sequence specificity of DUX4. *Skeletal muscle.* 2016; 6:8. doi: [10.1186/s13395-016-0080-z](https://doi.org/10.1186/s13395-016-0080-z) PMID: [26823969](https://pubmed.ncbi.nlm.nih.gov/26823969/)
17. Rickard AM, Petek LM, Miller DG. Endogenous DUX4 expression in FSHD myotubes is sufficient to cause cell death and disrupts RNA splicing and cell migration pathways. *Human molecular genetics.* 2015; 24(20):5901–14. Epub 2015/08/08. doi: [10.1093/hmg/ddv315](https://doi.org/10.1093/hmg/ddv315) PMID: [26246499](https://pubmed.ncbi.nlm.nih.gov/26246499/); PubMed Central PMCID: [PMC4581613](https://pubmed.ncbi.nlm.nih.gov/PMC4581613/).
18. Krom YD, Thijssen PE, Young JM, den Hamer B, Balog J, Yao Z, et al. Intrinsic Epigenetic Regulation of the D4Z4 Macrosatellite Repeat in a Transgenic Mouse Model for FSHD. *PLoS genetics.* 2013; 9(4):e1003415. Epub 2013/04/18. doi: [10.1371/journal.pgen.1003415](https://doi.org/10.1371/journal.pgen.1003415) PMID: [23593020](https://pubmed.ncbi.nlm.nih.gov/23593020/); PubMed Central PMCID: [PMC3616921](https://pubmed.ncbi.nlm.nih.gov/PMC3616921/).
19. Dandapat A, Bosnakovski D, Hartweck LM, Arpke RW, Baltgalvis KA, Vang D, et al. Dominant lethal pathologies in male mice engineered to contain an X-linked DUX4 transgene. *Cell Rep.* 2014; 8(5):1484–96. Epub 2014/09/02. doi: [10.1016/j.celrep.2014.07.056](https://doi.org/10.1016/j.celrep.2014.07.056) PMID: [25176645](https://pubmed.ncbi.nlm.nih.gov/25176645/); PubMed Central PMCID: [PMC4188423](https://pubmed.ncbi.nlm.nih.gov/PMC4188423/).
20. Fitzsimons RB, Gurwin EB, Bird AC. Retinal vascular abnormalities in facioscapulohumeral muscular dystrophy. A general association with genetic and therapeutic implications. *Brain.* 1987; 110 (Pt 3):631–48. Epub 1987/06/01. PMID: [3580827](https://pubmed.ncbi.nlm.nih.gov/3580827/).
21. Padberg GW, Brouwer OF, de Keizer RJ, Dijkman G, Wijmenga C, Grote JJ, et al. On the significance of retinal vascular disease and hearing loss in facioscapulohumeral muscular dystrophy. *Muscle & nerve.* 1995; 2:S73–80. Epub 1995/01/01. PMID: [7739630](https://pubmed.ncbi.nlm.nih.gov/7739630/).
22. Trevisan CP, Pastorello E, Tomelleri G, Vercelli L, Bruno C, Scapolan S, et al. Facioscapulohumeral muscular dystrophy: hearing loss and other atypical features of patients with large 4q35 deletions. *Eur J Neurol.* 2008; 15(12):1353–8. Epub 2008/12/04. doi: [10.1111/j.1468-1331.2008.02314.x](https://doi.org/10.1111/j.1468-1331.2008.02314.x) PMID: [19049553](https://pubmed.ncbi.nlm.nih.gov/19049553/).
23. Lyon MF. Gene action in the X-chromosome of the mouse (*Mus musculus* L.). 1961.
24. Cannon B, Nedergaard J. Nonshivering thermogenesis and its adequate measurement in metabolic studies. *J Exp Biol.* 2011; 214(Pt 2):242–53. Epub 2010/12/24. doi: [10.1242/jeb.050989](https://doi.org/10.1242/jeb.050989) PMID: [21177944](https://pubmed.ncbi.nlm.nih.gov/21177944/).
25. Webb GP, Jagot SA, Jakobson ME. Fasting-induced torpor in *Mus musculus* and its implications in the use of murine models for human obesity studies. *Comp Biochem Physiol A Comp Physiol.* 1982; 72(1):211–9. Epub 1982/01/01. PMID: [6124358](https://pubmed.ncbi.nlm.nih.gov/6124358/).

26. Hudson JW, Scott IM. Daily torpor in the laboratory mouse, *Mus musculus* var. albino. *Physiological Zoology*. 1979;205–18.
27. Blackstone E, Morrison M, Roth MB. H₂S induces a suspended animation-like state in mice. *Science*. 2005; 308(5721):518. Epub 2005/04/23. doi: [10.1126/science.1108581](https://doi.org/10.1126/science.1108581) PMID: [15845845](https://pubmed.ncbi.nlm.nih.gov/15845845/).
28. Bradford EM, Miller ML, Prasad V, Nieman ML, Gawenis LR, Berryman M, et al. CLIC5 mutant mice are resistant to diet-induced obesity and exhibit gastric hemorrhaging and increased susceptibility to torpor. *American journal of physiology Regulatory, integrative and comparative physiology*. 2010; 298(6):R1531–42. Epub 2010/04/02. doi: [10.1152/ajpregu.00849.2009](https://doi.org/10.1152/ajpregu.00849.2009) PMID: [20357015](https://pubmed.ncbi.nlm.nih.gov/20357015/); PubMed Central PMCID: [PMC2886706](https://pubmed.ncbi.nlm.nih.gov/PMC2886706/).
29. Inagaki T, Dutchak P, Zhao G, Ding X, Gautron L, Parameswara V, et al. Endocrine regulation of the fasting response by PPARalpha-mediated induction of fibroblast growth factor 21. *Cell Metab*. 2007; 5(6):415–25. Epub 2007/06/07. doi: [10.1016/j.cmet.2007.05.003](https://doi.org/10.1016/j.cmet.2007.05.003) PMID: [17550777](https://pubmed.ncbi.nlm.nih.gov/17550777/).
30. Greising SM, Baltgalvis KA, Kosir AM, Moran AL, Warren GL, Lowe DA. Estradiol's beneficial effect on murine muscle function is independent of muscle activity. *J Appl Physiol* (1985). 2011; 110(1):109–15. doi: [10.1152/jappphysiol.00852.2010](https://doi.org/10.1152/jappphysiol.00852.2010) PMID: [20966194](https://pubmed.ncbi.nlm.nih.gov/20966194/); PubMed Central PMCID: [PMC3253000](https://pubmed.ncbi.nlm.nih.gov/PMC3253000/).
31. Brouwer OF, Padberg GW, Ruys CJ, Brand R, de Laat JA, Grote JJ. Hearing loss in facioscapulohumeral muscular dystrophy. *Neurology*. 1991; 41(12):1878–81. Epub 1991/12/01. PMID: [1745341](https://pubmed.ncbi.nlm.nih.gov/1745341/).
32. Lutz KL, Holte L, Kliethermes SA, Stephan C, Mathews KD. Clinical and genetic features of hearing loss in facioscapulohumeral muscular dystrophy. *Neurology*. 2013; 81(16):1374–7. Epub 2013/09/18. doi: [10.1212/WNL.0b013e3182a84140](https://doi.org/10.1212/WNL.0b013e3182a84140) PMID: [24042093](https://pubmed.ncbi.nlm.nih.gov/24042093/); PubMed Central PMCID: [PMC3806909](https://pubmed.ncbi.nlm.nih.gov/PMC3806909/).
33. Hochedlinger K, Yamada Y, Beard C, Jaenisch R. Ectopic expression of Oct-4 blocks progenitor-cell differentiation and causes dysplasia in epithelial tissues. *Cell*. 2005; 121(3):465–77. PMID: [15882627](https://pubmed.ncbi.nlm.nih.gov/15882627/).
34. Perrin BJ, Strandjord DM, Narayanan P, Henderson DM, Johnson KR, Ervasti JM. beta-Actin and fascin-2 cooperate to maintain stereocilia length. *J Neurosci*. 2013; 33(19):8114–21. Epub 2013/05/10. doi: [10.1523/JNEUROSCI.0238-13.2013](https://doi.org/10.1523/JNEUROSCI.0238-13.2013) PMID: [23658152](https://pubmed.ncbi.nlm.nih.gov/23658152/); PubMed Central PMCID: [PMC3718021](https://pubmed.ncbi.nlm.nih.gov/PMC3718021/).
35. Speakman JR. Measuring energy metabolism in the mouse—theoretical, practical, and analytical considerations. *Front Physiol*. 2013; 4:34. doi: [10.3389/fphys.2013.00034](https://doi.org/10.3389/fphys.2013.00034) PMID: [23504620](https://pubmed.ncbi.nlm.nih.gov/23504620/); PubMed Central PMCID: [PMC3596737](https://pubmed.ncbi.nlm.nih.gov/PMC3596737/).
36. Schutz Y. On problems of calculating energy expenditure and substrate utilization from respiratory exchange data. *Z Ernährungswiss*. 1997; 36(4):255–62. PMID: [9467212](https://pubmed.ncbi.nlm.nih.gov/9467212/).
37. Ferrannini E. The theoretical bases of indirect calorimetry: a review. *Metabolism*. 1988; 37(3):287–301. PMID: [3278194](https://pubmed.ncbi.nlm.nih.gov/3278194/).